Compatibilization and Properties of EVA Copolymers Containing Surface-Functionalized Cellulose Microfibers

Mariano Pracella,* M. Minhaz-Ul Haque, Vera Alvarez

Cellulose microfibers were modified with two different bi-functional monomers. Composites of EVA copolymer with modified and unmodified cellulose were prepared by melt mixing. The samples were analyzed by SEM, XRD, FT-IR, DSC, TGA, DMTA and tensile mechanical tests. SEM showed that the presence of reactive groups on cellulose surface enhanced the compatibility, improving the fiber/matrix interfacial adhesion. FT-IR disclosed the occurrence of chemical reactions between the functionalized cellulose and polymer chains. The incorporation of fibers affected the crystallization behaviour and crystallinity of the polymer matrix. Composites with GMA modified cellulose displayed better compatibility, higher thermal and mechanical properties.

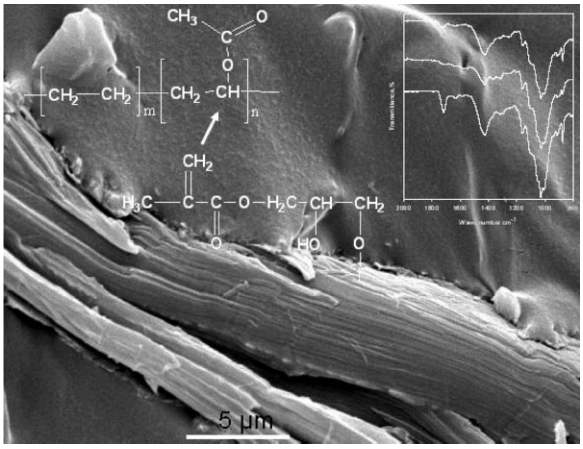

Introduction

Incorporation of natural fibers into synthetic polymers offers the possibility to design new class of composite materials with reduced environmental impact. When natural reinforced plastics are subjected, at the end of their life cycle, to a combustion process or landfill, the released amount of CO_2 of the fiber is neutral with respect to the assimilated amount during the growth.[1] Although natural fibers have many advantages, such as sustainability, recyclability, low density, biodegradability, low cost – which offer greater opportunities to develop a new class of environmentally friendly structural composites – the drawbacks for the application of cellulosic fibers are the strong hydrophilic nature of their surface, which causes poor adhesion and non-homogeneous dispersion in most non-polar matrices, as well as water absorbance, causing a decrease in the mechanical performances.[2,3] Indeed, high dispersion of fibers in the polymer matrix and good adhesion are important prerequisite for obtaining useful mechanical properties of the resulting composites, that can be achieved through suitable chemical/physical treatments.[4,5]

Many works have been carried out during the last decade on natural fiber-based polymer composites with polyolefin matrices [poly(propylene) (PP), polyethylene (PE), polystyrene

M. Pracella
Institute of Composite and Biomedical Materials, IMCB-CNR, Via Diotisalvi 2, Pisa 56122, Italy
Fax: +39 0502217866; E-mail: mariano.pracella@diccism.unipi.it
M. M. Haque
Department of Chemical Engineering and Materials Science, University of Pisa, Via Diotisalvi 2, Pisa 56122, Italy
V. Alvarez
Polymer Division, INTEMA-CONICET, University of Mar del Plata, Mar del Plata, Argentina

DOI: 10.1002/mame.201000175

(PS), etc.] and it has been reported that composites with modified fibers and/or polymer showed improved properties with respect to unmodified ones.[6–9] Poly[ethylene-*co*-(vinyl acetate)] (EVA) copolymers, due to their important rubber and resin properties,[10] are used for various applications, such as packaging films, adhesives/paper coatings, wire and cable insulation, barrier sheets, etc.[11] However, there exists only limited information about the properties of EVA-based composites. Dikobe and Luyt have examined composites of PP/EVA blends with wood powder (WP) and reported that WP influenced the crystallization behavior of EVA.[12] Mydul et al. have studied the mechanical properties of EVA and cellulose acetate (CA)-containing natural fibers (*Sterculia villosa*). They observed that the tensile strength of EVA composites decreased with the addition of fiber, whereas in CA composites, tensile strength increased due to the good distribution of fibers.[13] Malunka et al. have prepared EVA/sisal fiber composites by melt mixing in the presence of dicumyl peroxide (DCP) as a radical initiator, and mentioned that in presence of DCP grafting between EVA and sisal fiber took place. These composites were thermally more stable than both EVA and sisal fiber alone.[14] Espert et al. have studied PP/EVA/Technocel 165 (Cell) composites and reported that EVA improved the resistance of the composites to water absorption.[15] Moreover, EVA copolymers offer the possibility of preparing compatible blends with biodegradable polyesters [i.e., poly(lactic acid), PLA] which could be advantageously exploited for the preparation of composites with natural fillers.

To increase the compatibility among the composite components improving the interfacial adhesion and fiber dispersion, either surface modification of fibers and/or matrix, as well as addition of suitable copolymers can be exploited. Among the processes of chemical modification of natural fibers (such as alkaline, silane, permanganate treatments, or peroxidation, acetylation, benzoylation, etc.), those concerning grafting of maleic anhydride (MA)[5] and glycidyl methacrylate (GMA)[16] are very versatile. In particular, GMA functionalization has been used to effectively modify both the polymer matrix and natural fibers achieving enhanced interfacial bonding and mechanical properties of their composites.[8]

We investigated the preparation and characterization of EVA/Cell composites with components selectively modified by grafting of functional groups – able to improve the matrix/fiber interfacial interactions – in order to develop the performances and applications of eco-friendly materials based on natural fibers. In the present study, we report on the compatibilization of EVA/Cell composites by means of chemical modification of cellulose fibers with MA or GMA, aimed at analyzing the effect of functional groups and phase interactions on the morphological, structural, thermal and mechanical characteristics of these systems.

Experimental Part

Poly[ethylene-*co*-(vinyl acetate)] (EVA), trade name Elvax 220W, was supplied from DuPont, Italy. It contains 28% vinyl acetate and has a density of $0.951\,g\cdot cm^{-3}$, melt flow index (190 °C, 2.16 kg) = $150\,g\cdot(10\,min)^{-1}$ and melting point of 70 °C (technical data sheet). Cellulose powder, trade name Technocel 165 [cellulose content: 75%; density > $1.5\,kg\cdot dm^{-3}$; sieving: 125 μm (<20%), 32 μm (<80%)] was kindly supplied by Neuchem, Italy. These commercial fibers were used as received without any treatment; throughout this paper, Technocel 165 is referred to as Cell.

MA (purity min. 99.8%) was purchased from RPE, Italy. GMA, purity 97%, was purchased from Aldrich, Italy.

Cellulose Modification

Modification of cellulose with MA was carried out by addition of MA monomer ($0.5\,mol\cdot mol^{-1}$ of anhydrous glucose unit) into a cellulose/acetone suspension (1:10). The suspension was stirred for 8 h refluxing the solvent at 55 °C. The MA-modified cellulose (Cell-MA) was then cooled to room temperature, separated by filtration, washed with distilled water three times and finally with acetone, dried at 50 °C under vacuum and stored at 0 °C in a refrigerator.

Cellulose was functionalized with GMA following the procedure previously reported by Rozman et al.[16] 12 g of dried cellulose (Technocel 165) was reacted at 90 °C in batches with 60 mL of GMA/triethylamine (3:7 v/v) solution. To minimize the risk of free radical reaction at the unsaturated ends of GMA, hydroquinone (2 wt.-% of GMA) was added. After 4 h reaction, the modified cellulose was separated from the reagents by filtration, rinsed with acetone and refluxed with excess of fresh acetone for 4 h to ensure removal of solvent, unreacted reagents and GMA homopolymer formed during the reaction. After washing the treated cellulose was dried at 105 °C for 5 h under vacuum. The degree of substitution (DS) of GMA-modified cellulose (Cell-GMA) was determined according to the following protocol.[17] At room temperature, 300 mg of treated cellulose fibers were stirred in 10 mL of chloroform for 24 h under exclusion of light. A freshly prepared solution of bromine in chloroform was added to the mixer and stirred for more 2 h; finally 20 mL of methanol was added and filtered. The collected product was washed with 40 mL aqueous sodium thiosulfate (10% w/v), thrice with distilled water, thrice with methanol and dried at 40 °C under vacuum. The brominated cellulose (0.06033 g) was put in a fusion tube with sodium metal, fused and ground into water of a mortar. Then the solution was filtered, concentrated by evaporation, acidified with dilute HNO_3 and then $AgNO_3$ solution was added for precipitation as AgBr. The precipitate was separated and dried at 105 °C for 2 h and weighed. From the weight of Br, the DS of Cell-GMA was estimated.

Composite Preparation

Composites of modified and unmodified cellulose with EVA (80 wt.-% EVA, 20 wt.-% cellulose) were prepared in the presence of radical initiator bis[1-(*tert*-butylperoxy)-1-methylethyl]benzene (BTP) by melting in a Brabender Plasticorder internal mixer. The

Macromol. Mater. Eng. **2010**, *295*, 949–957

Macromolecular Journals
DOI: 10.1002/mame.201000175

composite components weighed according to the required ratio (total weight: 40 g) were mixed at 170 °C, at a mixing speed of 60 rpm for 10 min. Mixing torque moments were also recorded as a function of mixing time. Before mixing cellulose and polymer were dried under vacuum for 6 h at 90 and 60 °C, respectively. Composite EVA/Cell without initiator was also prepared. The composites were injection molded in oar shape by using a Proma WL-5 micro-injector (Torun, Poland) operating at 170/40 °C.

X-ray Diffraction

Wide-angle X-ray diffraction (XRD) of both pure and treated cellulose fibers was performed at room temperature with a Siemens Kristalloflex 810 diffractometer operating at 40 kV and 30 mA, using the Cu K_α radiation ($\lambda = 0.1546$ nm). The crystallinity degree of the fibers was determined as the ratio of the areas of crystalline reflections to the whole area (after subtraction of background) in the range $2\theta = 10$–50°.[18]

Scanning Electron Microscopy (SEM)

SEM analysis was made on the surfaces of injected composite samples freeze fractured in liquid nitrogen. The sample surfaces were sputter coated with fine layer of gold in an Edward Sputter Coater and analyzed by JEOL JSM-56000LV scanning electron microscopes. Average values of fiber length and diameter were measured with semi-automatic software (UTHSCSA Image Tool) from SEM micrographs. The average diameter and length of cellulose fibers were 17.5 and 189 μm, respectively (average fiber aspect ratio = 10.8).

DSC and Thermogravimetric Analysis (TGA)

DSC analysis was carried out in a Perkin-Elmer Pyris Diamond DSC under nitrogen stream. Samples (9–10 mg) were heated from 0 to 170 °C at a rate of 10 °C · min^{-1} and held at 170 °C for 2 min to eliminate the previous thermal history (first heating run), then they were cooled to 0 °C at 10 °C · min^{-1} and reheated under the same conditions to 170 °C (second heating run). Phase transition temperatures and enthalpies were recorded for each sample, respectively, from the maxima and areas of the crystallization and second run melting peaks.

TGA was carried out in a TGA Q500 analyzer. Samples (4–10 mg) were heated from 50 to 600 °C at 10 °C · min^{-1} both under nitrogen and air.

Fourier-Transform Infrared (FT-IR) Analysis

FT-IR analysis was performed by means of a Perkin-Elmer Spectrum One FT-IR spectrometer and a Perkin-Elmer Spotlight FT-IR imaging system. The samples were scanned in the frequency range 500–4 000 cm^{-1} at a resolution of 4 cm^{-1}. In case of EVA/Cell-MA and EVA/Cell-GMA the composite samples were dissolved in toluene and filtered by repeated steps, the fibers were then washed with acetone three times, and the dried cellulose residue were finally analyzed by FT-IR.

Dynamical Mechanical Analysis (DMTA)

DMTA was carried out by a Gabo Qualimeter Eplexor 100N (Germany) on injection molded samples. Glass transition temperature, T_g and tan δ values were calculated for all samples from DMTA analysis in the temperature range from −80 to +50 °C. The tests were carried out at a frequency of 1 Hz.

Mechanical Properties

Uniaxial tensile tests were carried out at room temperature (23 °C) in a universal testing machine at 50 mm · min^{-1} (Instron 4467) by following ASTM D 638M-93 standard recommendations. Dumbbell shaped specimens were used for these tests. Sample dimensions were measured to an accuracy of 0.01 mm. Stress/strain curves were obtained from these tests, and Young's modulus, tensile strength and elongation at break values were determined from these curves. At least three specimens were tested, and the average values were reported.

Rheological Tests

Measurements of rheological properties were performed using an MCR 301 Anton Paar with parallel-plate geometry rheometer. Tests were carried out in steady rate mode at 180 °C (molten state). Tests were done in a range of rates from 0.1 to 500 s^{-1}. For all experiments, the strain amplitude was maintained constant at 2%. Before starting dynamic frequency sweep tests, the linear viscoelastic range was determined through a strain sweep test. G' (storage modulus) and G'' (loss modulus) were registered as functions of deformation (γ). It was observed that G' and G'' remained constant until 3% of deformation, showing the linear viscoelastic range.

Results and Discussion

Characterization of Modified Cellulose

The morphology and structure of modified cellulose fibers were analyzed by SEM, FT-IR and WAXS analyses. Figure 1 represents the scanning electron micrographs of untreated Cell, Cell-MA and Cell-GMA, respectively. It is seen that the surfaces of both MA and GMA treated fibers as compared to the untreated fibers, show large roughness that could be ascribed to degradation effects during the treatment in solution.

In Figure 2, curves a, b and c represents the FT-IR spectra of Cell, Cell-MA and Cell-GMA, respectively. In the spectrum of Cell-MA an extra peak at 1 570 cm^{-1}, corresponding to the stretching of carboxylate COO group (due to the MA ring

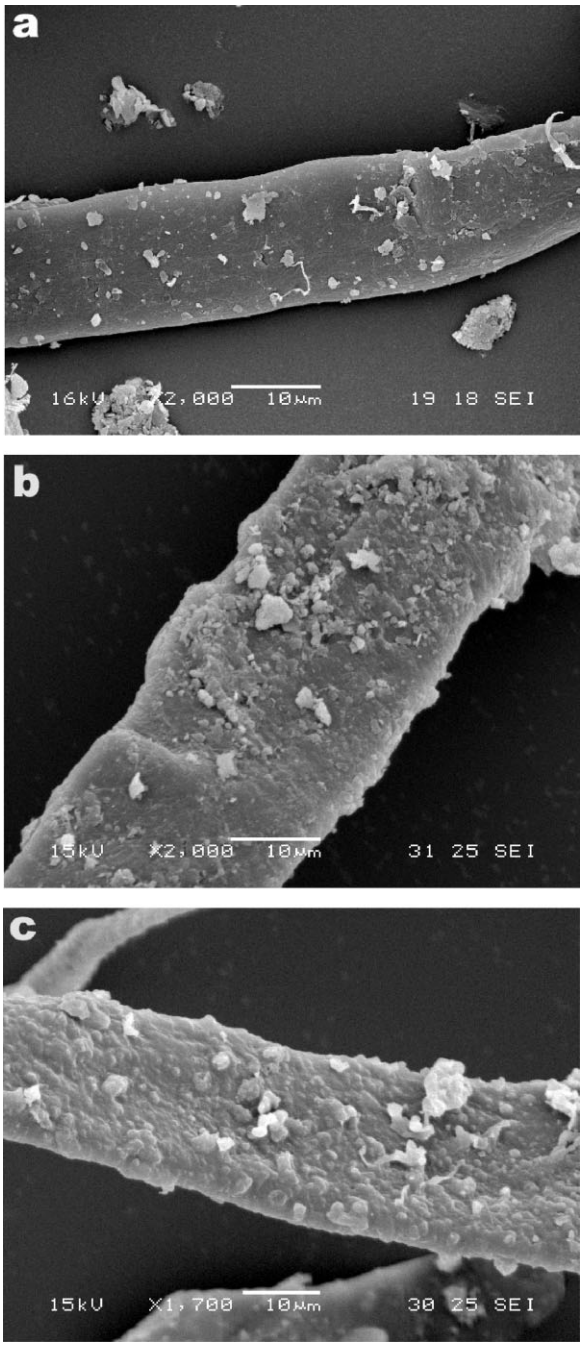

Figure 1. Scanning electron micrographs of (a) untreated, (b) MA treated and (c) GMA treated cellulose.

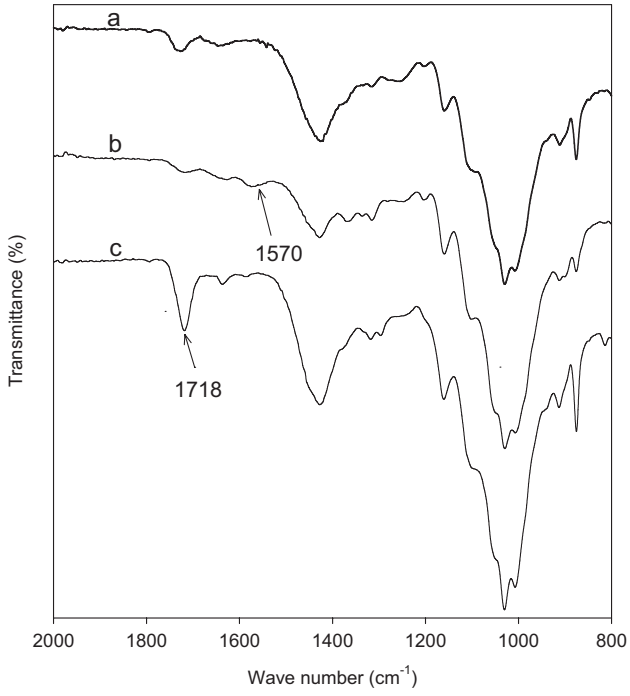

Figure 2. FT-IR spectra of (a) untreated, (b) MA treated and (c) GMA treated cellulose.

opening),[19] indicates that reaction between MA monomer and OH group of cellulose took place. On the other hand, in the spectrum of Cell-GMA, an intense carbonyl CO peak (corresponding to methacrylate) centered at 1 718 cm^{-1} is observed supporting the formation of bonding between the epoxy moiety of GMA and OH group of cellulose.[8] Figure 3 (step I) shows the reaction scheme for the grafting of GMA onto cellulose. The DS (=0.16) for GMA treated cellulose was calculated on the basis of elemental analysis.

X-ray diffraction patterns of both plain and treated fibers displayed characteristic peaks of crystalline cellulose at about 12.5, 15.8, 22.8 and 29.7° in the range $2\theta = 10–33°$ and other secondary peaks at higher 2θ values. The intensity of the peaks was affected by the chemical treatment and crystallinity decreased from 57% for unmodified Cell to 49%

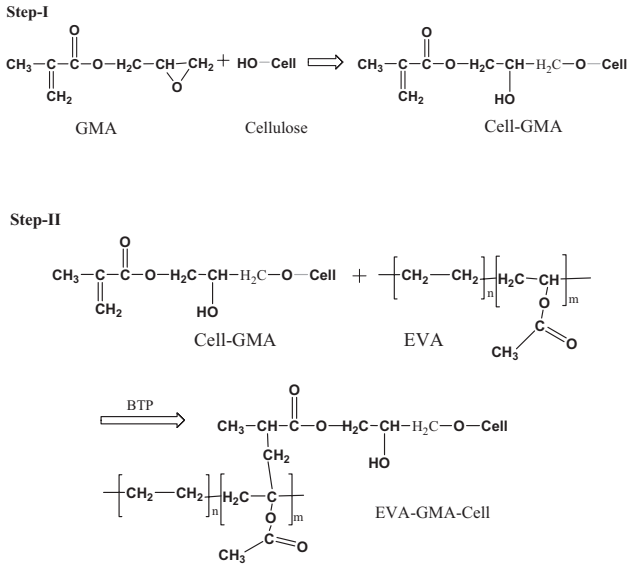

Figure 3. Reaction scheme.

Macromol. Mater. Eng. **2010**, *295*, 949–957

DOI: 10.1002/mame.201000175

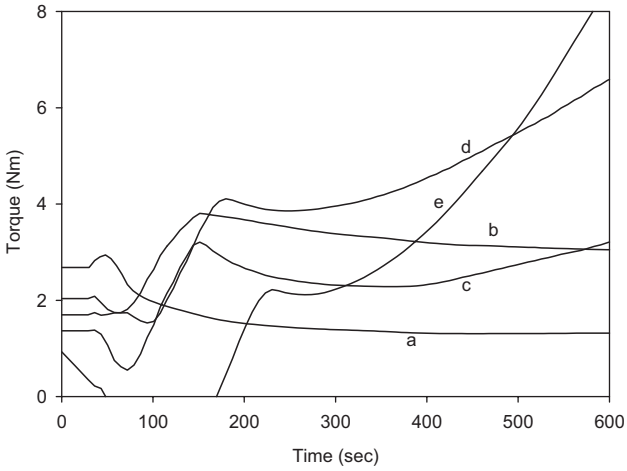

Figure 4. The torque response of (a) EVA (BTP), (b) EVA/Cell, (c) EVA/Cell-MA (BTP), (d) EVA/Cell-GMA (BTP) and (e) EVA/Cell (BTP) as function of mixing time.

in the case of Cell-GMA. Similar values of crystallinity, near to 49%, have been reported for microcrystalline cellulose particles by Eichhorn and Young.[18]

Mixing Torque of Composites

Figure 4 shows the torque response against time for EVA and EVA/Cell composites. It was found that in presence of initiator EVA alone did not exhibit increase of torque, whereas EVA/Cell, EVA/Cell-MA and EVA/Cell-GMA displayed a significant increase in torque as compared to EVA/Cell (without initiator). Larger values of torque were recorded for EVA/Cell-GMA respect to EVA/Cell-MA, indicating for the former system a more effective chemical reaction between the copolymer radicals and the double bond in functional groups of treated cellulose (see Figure 3, step II). This effect is supported by the melt viscosity data of the composites, as discussed in the next section. However, a rapid jump of torque was observed for EVA/Cell with BTP that can be related with the occurrence of cross-linking among copolymer chains, likely catalyzed by the cellulose fibers. To confirm the occurrence of cross-linking in the composites, solubility tests were carried out in toluene at room temperature. Insolubility of EVA/Cell (BTP) in toluene indicated that cross-linking took place in presence of initiator, whereas complete solubility was observed for EVA/Cell-MA and EVA/Cell-GMA which supported the chemical interactions between fiber and matrix.

SEM and FT-IR Analysis of Composites with Modified Cellulose

SEM micrographs of fracture surfaces of the examined composites are presented in Figure 5. It appears that the fracture surface of EVA/Cell (Figure 5a) shows poor polymer/fiber interfacial adhesion. Otherwise, the fracture surfaces of samples with functionalized cellulose (in presence of BTP) display good interfacial adhesion and the fiber surfaces are coated with a layer of polymer (Figure 5b and c) supporting an improved compatibility of treated cellulose with EVA copolymers. A similar effect has been observed for composites of PP with GMA modified Hemp fibers.[8]

Figure 6 shows the FT-IR spectra of EVA, Cell-GMA, and cellulose residue obtained after the polymer dissolution of EVA/Cell-GMA. The peaks at 2 920 and 2 850 cm^{-1} corresponding to the asymmetric C–H stretching in the EVA copolymer[12] (curve c) are also present in the spectrum of cellulose residue (curve b), indicating the existence of polymer on treated fibers. This observation can be considered as an evidence of chemical interaction between EVA and Cell-GMA, as represented in Figure 3 (step II) for the reaction of treated cellulose with the copolymer. Similarly, cellulose residue obtained from EVA/Cell-MA was also analyzed by FT-IR and no change was observed in the spectrum as compared to Cell-MA.

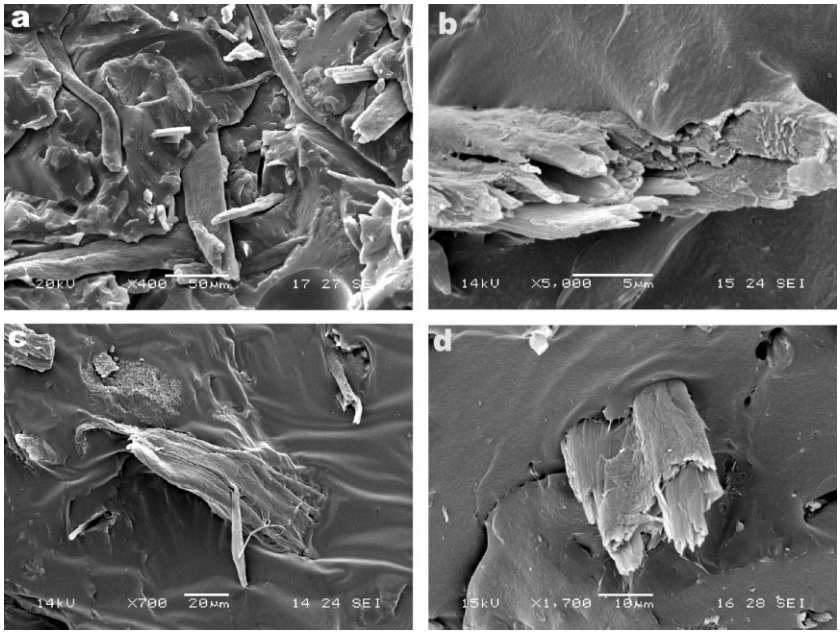

Figure 5. Scanning electron micrographs of composites (a) EVA/Cell, (b) EVA/Cell-MA (BTP), (c) EVA/Cell-GMA (BTP) and (d) EVA/Cell (BTP).

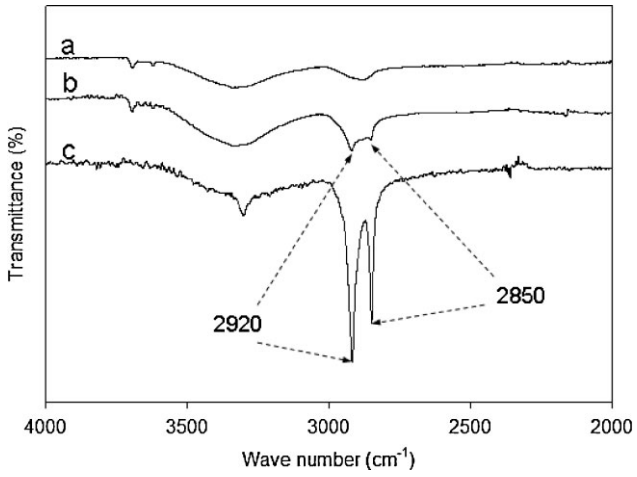

Figure 6. FT-IR spectra of (a) Cell-GMA, (b) cellulose residue obtained from EVA/Cell-GMA composite and (c) EVA.

Thermal Behavior

DSC cooling thermograms of EVA and its composites with treated and untreated cellulose are shown in Figure 7. The thermodynamic values of phase transitions are reported in Table 1. From Table 1 it is seen that the T_c of the EVA/Cell composite occurred at a slightly higher temperature as compared to EVA copolymer, suggesting a nucleating effect of cellulose on the crystallization of EVA matrix. The nucleating effect of fibers has been reported for several composite systems, such as PLA/microfibrillar cellulose,[20] PP/Hemp[8] and PLA containing various natural fibers.[21,22] Moreover, it can be noticed that the polymer crystallization enthalpy, ΔH_c, was significantly decreased by the fiber incorporation. On the other side, T_c of EVA/Cell-GMA and EVA/Cell-MA composites occurred at lower temperature as compared to EVA copolymer, probably due to the chemical interactions between modified cellulose and EVA

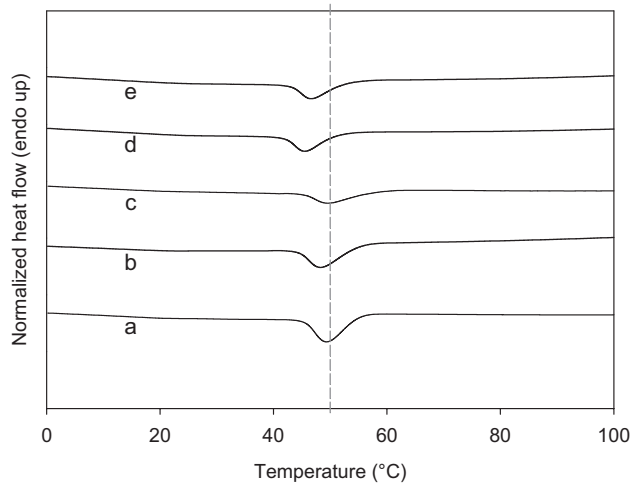

Figure 7. DSC cooling curve of (a) EVA, (b) EVA (BTP), (c) EVA/Cell, (d) EVA/Cell-GMA and (e) EVA/Cell-MA

Table 1. DSC and DMTA phase transition parameters of EVA and composites.

Sample	T_c	ΔH_c[a)]	T_g
	°C	J·g^{-1}	°C
EVA	48.3	15.9	−22.3
EVA (BTP)	48.6	12.1	−22.0
EVA/Cell	49.8	11.9	−19.4
EVA/Cell (BTP)	45.6	12.4	−18.2
EVA/Cell-GMA (BTP)	45.6	11.5	−19.4
EVA/Cell-MA (BTP)	46.9	10.9	−18.4

[a)]Enthalpy of crystallization per gram of polymer.

copolymer and to some cross-linking among EVA chains, which hinder the formation of polymer crystals.

Figure 8 shows the derivative thermogravimetric (DTG) curves of Cell, EVA, EVA/Cell, EVA/Cell-GMA and EVA/Cell-MA obtained in air. The peak temperatures of the various curves are summarized in Table 2. Both cellulose and EVA exhibited two decomposition steps. The weight loss of cellulose at 334 °C is due to the cleavage of the glucosidic linkages of cellulose.[23–26] In the case of EVA, the first step involves the degradation of VA groups, and the second one the degradation of the main chain.[14] In the curves of EVA/Cell, EVA/Cell-GMA and EVA/Cell-MA composites there are also two peaks, the first at 341–350 °C, which corresponds to the first thermal degradation of cellulose and EVA and the second at 444–458 °C, which corresponds to the second thermal degradation of cellulose and EVA. In each curve of composites, the first peak was shifted to higher temperature as compared to cellulose indicating that EVA copolymers most likely inhibit the oxidation of cellulose. It is important to notice that composites of EVA with GMA treated cellulose displayed higher thermal stability.

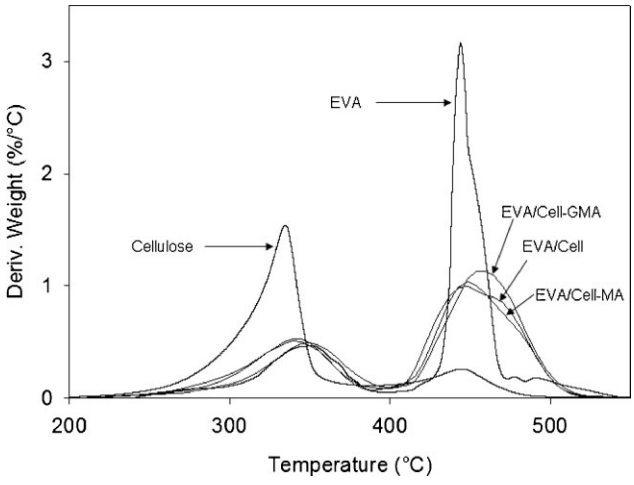

Figure 8. DTG curves cellulose, EVA and their composites.

Macromol. Mater. Eng. **2010**, *295*, 949–957

Macromolecular Journals

DOI: 10.1002/mame.201000175

Table 2. TGA degradation temperatures of Cell, EVA and their composites.

Sample	Degradation temperature	
	°C	
	First	Second
cellulose	334	445
EVA	350	443
EVA/Cell (BTP)	341	444
EVA/Cell-GMA(BTP)	350	458
EVA/Cell-MA (BTP)	340	448

DMTA

Figure 9 shows the effect of temperature on the tan δ value of pure EVA and its composites. Cellulose incorporation reduces the tan δ peak height by restricting the movement of the polymer molecules.[27] As reported in Table 1, the T_g of EVA increased somewhat in composites, supporting that the glass transition behavior of EVA matrix was affected by the incorporation of fibers. Chemical bonding at the interface can decrease the relaxational mobility in the polymer segments near the interface causing an increase in T_g, as it has been pointed out for some nanocomposites.[28]

Mechanical and Rheological Tests

The stress/strain curves recorded in the tensile test for pure EVA, BTP-treated EVA (EVA (BTP)) and their composites are shown in Figure 10. It is possible to observe that pure EVA exhibited an initial linear behavior followed by a nonlinear part, which indicates plastic deformation. When the initiator is added, the shape of the curve is quite similar but the nonlinear part is reduced indicating a decreased ductility. The incorporation of 20% cellulose produces a marked change on outline of the curve, minimizing the nonlinear part.

The values of Young's modulus, tensile strength and elongation at break obtained from mechanical tests are summarized in Table 3. Comparing pure EVA and EVA (BTP) it is clear that the use of initiator produce a decrease in both tensile strength and elongation at break. However, an increase on the stiffness may be related with the occurrence of cross-linking. When cellulose was incorporated into neat EVA, the rigidity of the material was quadruplicated, due to the higher modulus of cellulose respect to that of EVA, but the other properties were really reduced (about 60% in strength and 90% of elongation at break); whereas the reduction on the elongation at break is related with restrictions of the fibers to the matrix deformation, the drop of tensile strength can be associated to a lower fiber/matrix adhesion as verified by SEM microscopy (see Figure 5). On the other hand, when the initiator was used in addition to cellulose fibers, i.e., EVA/Cell (BTP), the increase in modulus was still higher and, although the elongation at break remained very low, the tensile strength was improved (37%) respect to pure EVA – and even more as compared to EVA/Cell – indicating an enhanced fiber/matrix interface, as demonstrated by SEM. MA treated cellulose contributed to the lesser decrease on elongation at break but the increase in modulus was lower and the tensile strength was again reduced (33%), demonstrating that the cross-linking may have a better effect on the mechanical properties than compatibility. The last case was the use of GMA treated cellulose: in that case, the tensile strength displayed a similar value of the pure matrix (both effects are compensated), whereas the modulus and elongation at break did not show any significant change with respect to MA-treated cellulose.

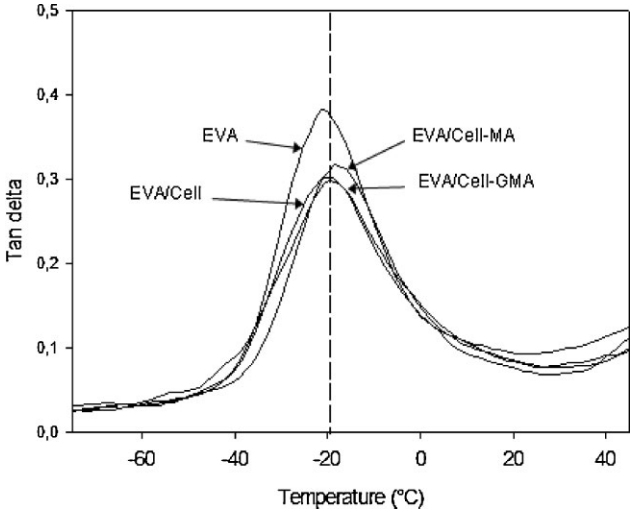

Figure 9. Effect of temperature on tan δ values of EVA/Cell composites.

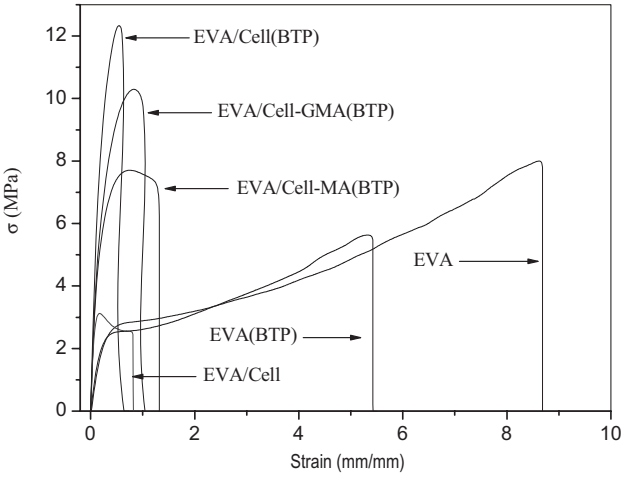

Figure 10. Stress/strain curves for pure EVA and composites obtained on tensile test.

Table 3. Tensile mechanical properties of EVA and composites.

Sample	σ_f	E	ε
	MPa	MPa	%
pure EVA	8.66 ± 1.32	10.7 ± 0.10	876.7 ± 50.3
EVA (BTP)	5.40 ± 0.33	12.9 ± 0.44	622.0 ± 102.16
EVA/Cell	3.40 ± 0.39	49.3 ± 4.41	69.7 ± 13.94
EVA/Cell (BTP)	11.92 ± 0.43	63.3 ± 16.85	65.9 ± 2.56
EVA/Cell-MA (BTP)	5.74 ± 0.55	42.9 ± 1.0	117.3 ± 1.59
EVA/Cell-GMA (BTP)	8.46 ± 1.36	45.9 ± 4.4	111.3 ± 11.8

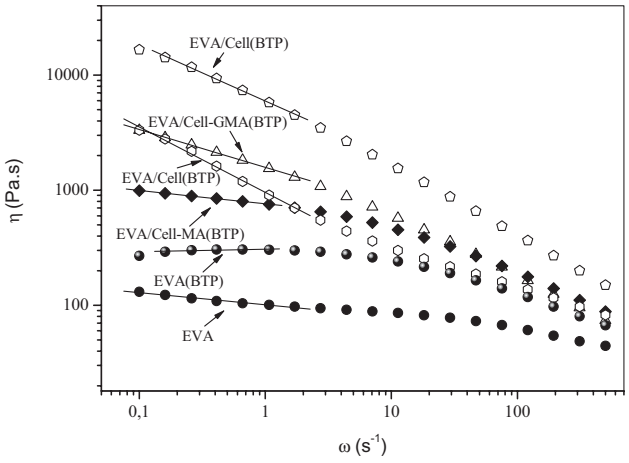

Figure 11. Viscosity as a function of frequency for EVA and EVA/Cell composites. Points represents experimental data and lines the application of power law model.

Table 4. Rheological properties of EVA and composites.

Sample	A_{Rh}	n_{Rh}
pure EVA	2.005	0.105
EVA (BTP)	2.487	0.000
EVA/Cell	2.981	0.568
EVA/Cell (BTP)	3.775	0.489
EVA/Cell-GMA (BTP)	3.198	0.329
EVA/Cell-MA (BTP)	2.882	0.116

Values of melt viscosity of composites are plotted in Figure 11 as a function of shear rate. The melt rheology curves were fitted to the classical power law expression:[29]

$$\eta = A_{Rh}\omega^{(n_{Rh})} \quad (1)$$

where the subscript Rh represents a rheological parameter, η is the apparent viscosity, A_{Rh} the preexponential factor, ω the oscillation frequency of the rheometer equivalent to shear rate and n_{Rh} is the shear thinning exponent. In the double logarithmic plot a linear zone at low shear rates can be seen. As reported in Table 4, the decrease in n_{Rh} indicates a more pseudoplastic character. Pure EVA together with EVA (BTP)- and EVA/Cell-MA (BTP) exhibited a clear pseudoplastic behavior (very low n_{Rh}). On the other hand, for EVA/Cell-GMA (BTP) and EVA/Cell (BTP) showed a pseudo-solid-like behavior with a pronounced shear thinning parameter. In these cases, Newtonian behavior disappeared at low frequency, suggesting a transition from liquid-like to solid-like viscoelastic behavior. The rheological behavior of neat EVA and EVA (BTP) exhibits the characteristic two regions: a Newtonian region at low frequency ($<0.1\,s^{-1}$) and shear thinning region at high frequency ($>1\,s^{-1}$). It is apparent that cellulose fibers have a dramatic effect on the rheological behavior. As 20% of fibers are added into the polymer matrix, the Newtonian region of the composites disappears and only the shear thinning region remains at the frequency from 0.01 to $100\,s^{-1}$.

Conclusion

The influence of modification of cellulose microfibers with bi-functional monomers (MA and GMA) on the properties of EVA/Cell composites was examined. It was shown that the morphology, as well as thermal, rheological and mechanical properties of the composites were significantly affected by the functionalized fibers. SEM analysis pointed out that the presence of reactive groups on cellulose surface enhanced the compatibility, improving the fiber/matrix interfacial adhesion as compared to unmodified EVA/Cell composites. This was correlated with the occurrence of chemical reactions between the double bond of MA and GMA groups onto cellulose and the polymer chains, as demonstrated by FT-IR analysis. All results – and mainly thermal and mechanical data – pointed out the superior performance of EVA/Cell-GMA composites, which can be accounted for by enhanced polymer/fiber interactions at the interface. Composites with GMA modified cellulose displayed improved interfacial adhesion, higher thermal

Macromol. Mater. Eng. **2010**, *295*, 949–957

Macromolecular Journals
DOI: 10.1002/mame.201000175

stability, good elongation at break and tensile strength as compared to EVA/Cell.

Finally, it is worth nothing to mention that modification of EVA copolymer with MA or GMA can also markedly influence the properties of EVA/Cell composites. As it has been previously discussed for composites with modified cellulose, the presence of reactive groups on the polymer matrix promoted the compatibilization of EVA/Cell, improving the interfacial adhesion.[30] The results of both thermal and mechanical analysis pointed out that GMA-modified EVA (EVA-GMA) gave rise to more effective polymer/fiber interactions with respect to MA modified EVA (EVA-MA).

Acknowledgements: The research was carried out in the frame of the *Agreement of Scientific Cooperation* between *CNR* (Italy) and *CONICET* (Argentina) 2009/2010.

Received: April 21, 2010; Published online: August 16, 2010; DOI: 10.1002/mame.201000175

Keywords: cellulose fibers; compatibilization; composites; ethylene vinyl acetate (EVA); interface interactions

[1] A. K. Bledzki, J. Gassan, *Prog. Polym. Sci.* **1999**, *24*, 221.
[2] A. K. Mohanty, M. A. Khan, G. Hinrichsen, *Compos. Sci. Technol.* **2000**, *60*, 1115.
[3] V. A. Alvarez, A. Vázquez, *Compos. Part A* **2006**, *37*, 1672.
[4] L. Jue, P. Askeland, T. D. Lawrence, *Polymer.* **2008**, *49*, 1285.
[5] N. Saheb, J. P. Jog, *Adv. Polym. Technol.* **1999**, *18*, 351.
[6] X. Li, G. Lope, P. Satyanarayan, *J. Polym. Environ.* **2007**, *15*, 25.
[7] J. B. Naik, S. Mishra, *Polym. Plast. Technol.* **2007**, *48*, 537.
[8] M. Pracella, D. Chionna, I. Anguillesi, Z. Kulinski, E. Piorkowska, *Compos. Sci. Technol.* **2006**, *66*, 2218.
[9] M. Pracella, C. Pancrazi, A. D'Alessio, A. Corti, E. Chiellini, *13th European Conference on Composite Materials*, June 2–5, 2008, Stockkolm, Sweden.
[10] J. Yin, J. Zhang, Y. Yao, *J. Appl. Polym. Sci.* **2006**, *102*, 841.
[11] M. A. Henderson, *IEEE Electr. Insul. Mag.* **1993**, *9*, 30.
[12] D. G. Dikobe, A. S. Luyt, *Express Polym. Lett.* **2009**, *3*, 190.
[13] M. A. Mydul, T. Ahmed, M. M. Haque, M. A. Gafur, H. A. N. M. Kabir, *Polym. -Plast. Technol.* **2009**, *48*, 101.
[14] M. E. Malunka, A. S. Luyt, H. Krump, *J. Appl. Polym. Sci.* **2006**, *100*, 1607.
[15] A. Espert, F. Vilaplana, S. Karlsson, *Compos. Part A* **2004**, *35*, 1267.
[16] H. D. Rozman, R. N. Kumar, H. P. S. Khalil, A. Abusamah, R. Abu, *Eur. Polym. J.* **1997**, *33*, 1213.
[17] H. Thomas, L. Thorger, F. Dominik, K. Andreas, *Polym. Bull.* **2008**, *61*, 1.
[18] S. J. Eichhorn, R. J. Young, *Cellulose* **2001**, *8*, 197–207.
[19] K. Nakanishi, *Infrared Absorption Spectroscopy*, Holden-Day, Inc., San Francisco and Nankodo Com Ltd., Tokyo 1962, p. 44.
[20] L. Suryanegara, A. N. Nakagaito, H. Yano, *Compos. Sci. Technol.* **2009**, *69*, 1187.
[21] R. Masirek, Z. Kulinski, D. Chionna, E. Piorkowska, M. Pracella, *J. Appl. Polym. Sci.* **2007**, *105*, 255.
[22] E. Lezak, Z. Kulinski, R. Masirek, E. Piorkowska, M. Pracella, K. Gadzinowska, *Macromol. Biosci.* **2008**, *8*, 1190.
[23] M. Wollerdorfer, H. Bader, *Ind. Crops Prod.* **1998**, *8*, 105.
[24] C. Albano, J. Gonzalez, M. Ichazo, D. Kaiseer, *Polym. Degrad. Stab.* **1999**, *66*, 170.
[25] N. Marcovich, M. M. Reboredo, M. I. Aranguren, *Thermochim. Acta* **2001**, *372*, 45.
[26] V. A. Alvarez, A. Vázquez, *Polym. Degrad. Stab.* **2004**, *84*, 13.
[27] L. A. Pathan, Z. Oommn, S. Thomas, *Compos. Sci. Technol.* **2003**, *63*, 283.
[28] W. K. Goertzen, M. R. Kessler, *Compos. Part A* **2008**, *39*, 761.
[29] T. W. Spriggs, J. D. Huppler, R. B. Bird, *Trans. Soc. Rheol.* **1966**, *10*, 191.
[30] M. M. Haque, M. Pracella, *Compos. Part A* (to be published, DOI: 10.1016/j.compositesa.2010.07.001)